Electrochimica Acta 317 (2019) 542–550

Contents lists available at ScienceDirect

Electrochimica Acta

journal homepage: www.elsevier.com/locate/electacta

Thermodiffusion of sodium polystyrene sulfonate in a supporting electrolyte

Miikka Jokinen [a], José A. Manzanares [b], Lasse Murtomäki [a, *]

[a] Department of Chemistry and Materials Science, School of Chemical Engineering, Aalto University, P.O. Box 16100, FI-00076, Aalto, Finland
[b] Department of Earth Physics and Thermodynamics, University of Valencia, E-46100, Burjassot, Spain

ARTICLE INFO

Article history:
Received 23 February 2019
Received in revised form
29 May 2019
Accepted 29 May 2019
Available online 1 June 2019

Keywords:
Soret effect
Thermodiffusion
Polyelectrolyte
Non-isothermal process

ABSTRACT

Thermodiffusion, or the Soret phenomenon, is well understood in simple systems, but in multicomponent and polyvalent electrolyte systems the process becomes more complicated due to the coupling of fluxes. We experimentally investigate the time evolution of a concentration gradient generated by thermodiffusion of a polyelectrolyte (poly(sodium 4-styrene sulfonate), NaPSS) in a 1:1 supporting electrolyte. We also derive and solve the transport equations that are used to extract the Soret coefficient from the experimental observations. It is shown that NaPSS thermodiffusion in NaCl is strongly dependent on concentration, with almost 100% thermal separation in concentrations below 15 nmol L^{-1}. Moreover, the results suggest that the supporting electrolyte can greatly influence the thermodiffusion of the polyelectrolyte, in some cases possibly even reversing the direction of the flux from the usual case of enrichment at the cold side.

1. Introduction

The tendency of a solute to move along a temperature gradient is known as thermodiffusion [1,2]. The process occurs because the heat flux induced by the temperature gradient is coupled with the solute flux, thus creating a concentration gradient even in a system with an initially uniform concentration [2]. In a closed system, the concentration gradient increases until an equilibrium state is reached when diffusion to the opposite direction cancels out the thermodiffusion [1]. In this equilibrium state, the solute flux density vanishes and $\vec{\nabla}\ln c = -\sigma_T \vec{\nabla} T$, where c is the solute concentration, σ_T is its Soret coefficient, and T is the temperature [1]. Thus, a thermophobic solute with positive Soret coefficient is enriched at cold locations.

A strong interest in thermodiffusion stems from its application to the study of macromolecules [3]. The tendency of the particles to move in the temperature field is more pronounced when the particles are larger, a feature that can be applied to separate molecules, nanoparticles and colloids [3,4], but it finds use in other applications as well. Thermodiffusion has been used to analyze the size of the particles [5], to tune the local concentration of the involved species [4], and to investigate the interactions between the solvent and the solute [6,7]. Also, it can be used to analyze the critical micelle concentration of surfactant solutions, and to estimate the effective charge of macromolecules [3]. Furthermore, it plays a role in natural phenomena such as component segregation in Earth's mantle and oceans [8,9], and even its role in the origin of life has been speculated [10–12].

Thermodiffusion in simple systems, such as aqueous 1-1 electrolytes [13–15], neutral molecules and liquid mixtures [16–18], polymers [19–21], and surfactants and colloids in different solvents [22–24] has been covered extensively in the literature. Generally, the Soret coefficient decreases with concentration, and increases with size of the solute [21]. For many polymers, the Soret coefficient reportedly depends on molar mass $\sigma_T \sim M^a$ where $a = 0.5–0.8$ [25]. However, when the system becomes more complex, understanding the phenomenon properly has appeared to be difficult [26]. The thermodiffusion characteristics of polyelectrolytes are very different from neutral polymers [23], as their strongly non-ideal behavior in multicomponent systems complicates the analysis [26]. Results from different studies on polyelectrolytes underline these complexities. Agar and Lobo [27], and later Lobo and Teixeira [28] studied sodium polyacrylates with different molecular weights and reported that the Soret coefficient is roughly proportional to the number of monomer units in the polyelectrolyte. This seemingly contradicts the reports of Snowdon and Turner [14], who

* Corresponding author.
E-mail address: lasse.murtomaki@aalto.fi (L. Murtomäki).

https://doi.org/10.1016/j.electacta.2019.05.155
0013-4686/

found that the additivity rule does not apply to multivalent electrolytes. Leaist and Hao [29] measured separately the Soret coefficients of aqueous NaPSS (poly(sodium-4-styrenesulfonate)) and aqueous NaCl, and deducted from these measurements that adding NaCl as a supporting electrolyte to dilute aqueous NaPSS would significantly increase the thermal separation of the polyelectrolyte. However, they were unable to verify their prediction experimentally. Such enhancement of the Soret effect seems to be the effect of the polyelectrolyte, as similar behavior has not been reported for smaller ions in supporting electrolytes [30].

In this paper, we investigate the nonstationary thermodiffusion of NaPSS in aqueous salt solutions. The growing interest in macromolecule thermodiffusion, especially in biologically relevant solutions, requires a thorough understanding of the Soret phenomenon in multicomponent systems, thus making this research timely and relevant. In the final equilibrium state, the concentration gradient of NaPSS satisfies $\vec{\nabla}\ln c = -\sigma_T^*\vec{\nabla}T$, where σ_T^* is its Soret coefficient in the mixture. The asterisk signifies that this coefficient depends on the mixture composition and differs from the Soret coefficient of NaPSS in absence of added salt. However, the analysis of experimental results of nonstationary thermodiffusion cannot make use of the simple expression $\vec{\nabla}\ln c = -\sigma_T^*\vec{\nabla}T$, as it is restricted to steady state. Therefore, we derive here the thermodiffusion theory for the mixture of a trace polyelectrolyte (NaPSS) and a supporting electrolyte. Our results show how the observed thermal separation of NaPSS in a supporting electrolyte, and its Soret coefficient in the mixture, change with the polyelectrolyte concentration, and how the choice of supporting electrolyte affects the thermal separation.

2. Theory

The molar flux density $\vec{J}_{13}$ of an electrolyte $A_{\nu_1}C_{\nu_{3,1}}$ (index 13) in aqueous solution due to concentration and temperature gradients is

$$-\vec{J}_{13} = D_{13}\left(\vec{\nabla}c_{13} + \sigma_{T,13}c_{13}\vec{\nabla}T\right), \tag{1}$$

where c_{13} is the concentration, D_{13} is the diffusion coefficient and $\sigma_{T,13}$ is the Soret coefficient. When transport takes place inside an ion-exchange membrane, its surface charge may give rise to thermoosmosis, the transport of solvent due to the temperature gradient. Thermoosmosis, however, does not occur or is negligible in non-charged membranes with relatively large pores [31,32], such as the glass frit used in this study.

In a mixture of strong electrolytes $A_{\nu_1}C_{\nu_{3,1}}$ (index 13) and $B_{\nu_2}C_{\nu_{3,2}}$ (index 23) sharing a common ion, the transport of one electrolyte is also affected by the concentration gradient of the other. Thus, the molar flux density of the electrolyte 23 is

$$-\vec{J}_{23} = D_{23,13}\vec{\nabla}c_{13} + D_{23,23}\vec{\nabla}c_{23} + D_{T,23}^*c_{23}\vec{\nabla}T, \tag{2}$$

where $D_{23,13}$ and $D_{23,23}$ are the diffusion coefficients and $D_{T,23}^*$ is the thermodiffusion coefficient. Again, the asterisk indicates value in a mixture. The Nernst-Planck approximation of ion transport allows deriving relationships between these coefficients and the ionic diffusion and thermodiffusion coefficients (see Appendix).

If electrolyte 23 is a trace component and 13 is a supporting electrolyte, the flux density of electrolyte 13 is given by eq (1) and it is not affected by electrolyte 23. In this case, the coefficient $D_{23,23}$ is equal to the diffusion coefficient D_2 of the ionic species 2 and $D_{23,13}$ is proportional to D_2 and to the concentration ratio, namely $D_{23,13} = \alpha D_2 c_{23}/c_{13}$ where α is a proportionality constant (see Appendix) [33]. Since $c_{23} \ll c_{13}$, this coefficient is close to zero and the coupling of fluxes is insignificant. Eliminating $\vec{\nabla}c_{13}$ from eqs (1) and (2) we get

$$-\vec{J}_{23} + \frac{D_{23,13}}{D_{13}}\vec{J}_{13} = D_2\left(\vec{\nabla}c_{23} + \sigma_{T,23}^*c_{23}\vec{\nabla}T\right), \tag{3}$$

where $\sigma_{T,23}^* = D_{T,23}^*/D_2 - \alpha\sigma_{T,13}$ is the Soret coefficient of the electrolyte 23 in the mixture. When the Soret equilibrium distribution is achieved between two chambers α and β at different temperatures (Fig. 1), $J_{13} = J_{23} = 0$, and the Soret coefficient can be calculated from the concentrations in the chambers as [29].

$$\sigma_{T,23}^* = -\left(\frac{\ln(c_{23}^\beta/c_{23}^\alpha)}{T^\beta - T^\alpha}\right)_{J_{13}=J_{23}=0}. \tag{4}$$

A positive value of $\sigma_{T,23}^*$ results in the accumulation of electrolyte 23 at the cold chamber, a behavior referred to as thermophobic.

We seek to measure the Soret coefficient $\sigma_{T,23}^*$ of a trace polyelectrolyte $BC_{\nu_{3,2}}$ (23) mixed with a 1-1 supporting electrolyte AC (13). The Soret coefficient $\sigma_{T,23}^*$ in the mixture differs from its value $\sigma_{T,23}$ in absence of supporting electrolyte because the transport of the polyelectrolyte ion is affected by the supporting electrolyte through the thermodiffusion potential. As shown in the Appendix, the relation between $\sigma_{T,23}^*$ and $\sigma_{T,23}$ is

$$\sigma_{T,23}^* \approx \sigma_{T,23} + \nu_{3,2}\left(\sigma_{T,23} - \sigma_{T,13}\right), \quad (c_{23} \ll c_{13}). \tag{5}$$

The Soret coefficient $\sigma_{T,13}$ of the supporting electrolyte is known from the literature, as the trace assumption imposes that it is not affected by the trace electrolyte 23. Noteworthy, $\sigma_{T,23}^*$ does not depend on the concentrations c_{13} and c_{23}. Since the stoichiometric coefficient $\nu_{3,2}$ is much larger than unity, $\sigma_{T,23}^*$ can be very different from $\sigma_{T,23}$. In particular, very large Soret coefficients $\sigma_{T,23}^*$ can be observed [29] when $\sigma_{T,23} > \sigma_{T,13}$ and $\nu_{3,2} \gg 1$.

We analyze the time evolutions of the concentrations $c_{23}^\alpha(t)$ and $c_{23}^\beta(t)$, rather than the equilibrium values as in eq (4). Since $J_{13} \neq 0 \neq J_{23}$, the concentrations $c_{23}^\alpha(t)$ and $c_{23}^\beta(t)$ must be calculated from the solution of eqs (1) and (3). The supporting electrolyte diffuses much faster than the large polyelectrolyte [29], and hence it can be assumed (see Appendix, eq (A12) onwards) that it has reached the Soret equilibrium distribution, $J_{13} \approx 0$, while the polyelectrolyte concentration is still evolving. Then, eq (3)

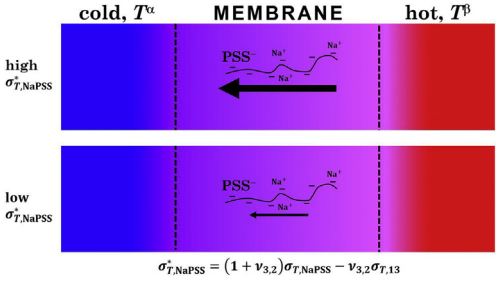

Fig. 1. The polyelectrolyte (NaPSS) flows in a 1-1 supporting electrolyte (13) through a membrane that separates two chambers, α and β, at temperatures T^α and T^β and identical initial composition. The temperature difference induces a separation of NaPSS that is determined by its Soret coefficient $\sigma_{T,NaPSS}^*$ in the mixture. This coefficient can be related to the Soret coefficients $\sigma_{T,NaPSS}$ and $\sigma_{T,13}$ of the polyelectrolyte and supporting electrolyte, respectively, and to the stoichiometric coefficient $\nu_{3,2}$ of sodium in the polyelectrolyte.

simplifies to

$$-\vec{J}_{23} \approx D_2\left(\vec{\nabla}c_{23} + \sigma^*_{T,23}c_{23}\vec{\nabla}T\right), \quad (J_{13} \approx 0). \tag{6}$$

The thermodiffusion experiments last for several days and the evaporation of water has an effect on the concentrations, especially because we measure rather slight concentration changes. Evaporation might easily be misunderstood as the system still being out of the Soret equilibrium, because it slowly changes the concentrations. To account for these changes, the compartment volumes V^α and V^β are

$$V^\alpha(t)\,/\,V^\alpha_0 = V^\beta(t)/V^\beta_0 = 1 - \omega t \tag{7}$$

where V^α_0 and V^β_0 are the initial volumes and ω is the evaporation rate. The total concentration change can then be thought to be due to thermodiffusion and the slow evaporation of water.

The transport of a species i ($i = 13, 23$) through a membrane that separates two chambers α and β is subject to the (amount) conservation law

$$\frac{\mathrm{d}(V^\alpha c^\alpha_i)}{\mathrm{d}t} = -AJ_i \tag{8}$$

where A is the membrane area. Conservation also implies $V^\alpha c^\alpha_i + V^\beta c^\beta_i = (V^\alpha_0 + V^\beta_0)c_{i,0}$, where $c_{i,0}$ is the initial concentration, so that

$$c^\beta_i = \frac{V^\alpha_0}{V^\beta_0}\frac{(V^\alpha_0 + V^\beta_0)c_{i,0} - V^\alpha c^\alpha_i}{V^\alpha}. \tag{9}$$

Here, the volume of the diaphragm (membrane) is assumed negligible. When the rate of solute transport through the membrane is fast compared to the rate of concentration change in the chambers, the quasi-steady state approximation can be conveniently used [33]. That is, the flux density J_i can be considered to be independent of position, although the concentrations $c_i(0,t) = c^\alpha_i(t)$ and $c_i(h,t) = c^\beta_i(t)$, and hence $c_i(x,t)$, are slowly varying with time.

Transport takes place across a neutral membrane of thickness h and the temperature profile can be assumed to be linear, so that $(\partial T/\partial x)_t = \Delta T/h$, where $\Delta T = T^\beta - T^\alpha$. The polyelectrolyte flux density is

$$J_{23} = -D_2\left(\left(\frac{\partial c}{\partial x}\right)_t + c\frac{\sigma^*_{T,23}\Delta T}{h}\right), \tag{10}$$

where we have dropped subscript 23 on c. The diffusion coefficient actually depends on temperature, but it can be estimated that using an average value for D_2 in the range 298–318 K the error is only of the order of 1%, compared to the case that D_2 depends linearly on temperature. Thus, the assumption of a constant, average value of D_2 can be accepted.

The flux density J_{23} can be expressed in terms of the polyelectrolyte concentrations c^α and c^β in the chambers by integration of eq (10) with respect to x. Elimination of c^β using eq (9) and integration of eq (8) with respect to t gives

$$c^\alpha(t) = \frac{c^\alpha_\infty + (c_0 - c^\alpha_\infty)(1-\omega t)^{1/(\omega\tau_{23})}}{1-\omega t}. \tag{11}$$

In the absence of evaporation, the equilibrium concentration would be

$$c^\alpha_\infty = \frac{V^\alpha_0 + V^\beta_0}{V^\alpha_0 + V^\beta_0 \mathrm{e}^{-\sigma^*_{T,23}\Delta T}}c_0 \tag{12}$$

and eq (11) would reduce to $c^\alpha = c^\alpha_\infty + (c_0 - c^\alpha_\infty)\mathrm{e}^{-t/\tau_{23}}$. As expected, eqs (9) and (12) imply $\ln(c^\beta_\infty/c^\alpha_\infty) = -\sigma^*_{T,23}\Delta T$. The relaxation time τ_{23} is given by

$$\frac{1}{\tau_{23}} = \frac{AD_2E_{T,23}}{h}\left(\frac{\mathrm{e}^{-\sigma^*_{T,23}\Delta T}}{V^\alpha_0} + \frac{1}{V^\beta_0}\right) \tag{13}$$

where $E_{T,23} = \sigma^*_{T,23}\Delta T/(1 - \mathrm{e}^{-\sigma^*_{T,23}\Delta T})$ is the thermophoretic enhancement factor, analogous to the iontophoretic enhancement factor [33]. Transport is enhanced, $E_{T,23} \geq 1$, when $\sigma^*_{T,23}\Delta T \geq 0$.

3. Experimental

The poly(sodium-4-styrenesulfonate) ($M = 500$ kg/mol, i.e. $Na_{2400}PSS$, Alfa Aesar, USA) solutions in a 0.1 mol L^{-1} supporting electrolyte were prepared in distilled and purified water (Milli-Q, Millipore, USA). The studied supporting electrolytes include NaCl, $NaClO_4$, Na_2SO_4, and LiCl. A standard diffusion cell (Side-bi-Side, Permegear, USA) was used (Fig. 2). It comprised of two half-cells which could be set to different temperatures with outer water jackets connected to thermostats. The half-cells had 10 mm round apertures, between which a porous fritted glass (Laborexin Oy, Finland) could be tightened and sealed. The glass frit had a thickness of 4 mm, and according to the information provided by the manufacturer, its pore size was in the range 40–100 μm. The pore size, together with the low porosity of the frit prevented mixing through the membrane. The temperature difference over the membrane was measured with thermocouples close to the membrane surface on both sides.

The α-side of the cell was connected to a flow-through UV/Vis cuvette and the electrolyte circulated through a spectrophotometer (Cary 60 UV–Vis, Agilent USA) by a peristaltic pump (IPS, Ismatec

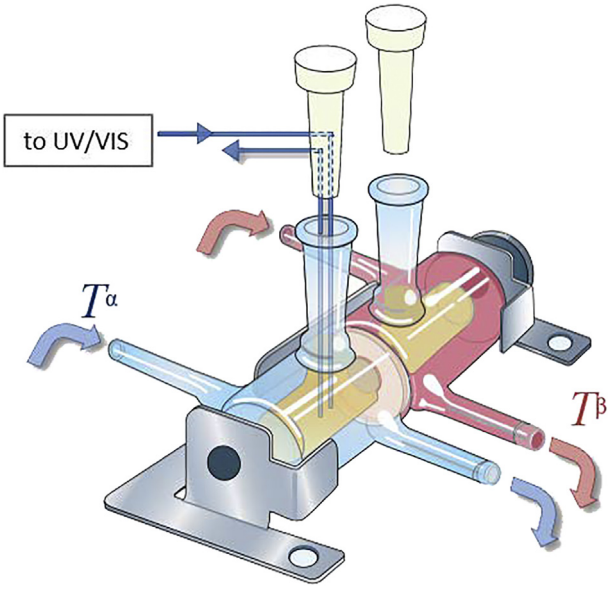

Fig. 2. The Side-bi-Side diffusion cell consists of two compartments of 3 mL, which can be set to different temperatures. Magnetic bars stir both sides. The total volume of the cold side (α) when connected to a flow-through cuvette is 5 mL. Modified with permission from Ref. [34].

Germany) with a flow rate of 2 mL/min. The concentration of the polyelectrolyte was measured with absorbance of the solution in the wavelength range of 220–350 nm. The resulting spectrum showed two peaks, a highly sensitive one at 225 nm and the other at 262 nm. The former was used in analysis by calibrating the absorbance with known concentrations of polyelectrolyte. The spectrum was measured every 5 min for time $t = 0$–120 min, every 15 min for $t = 120$–360 min, and every 30 min for $t = 360$–7999 min, after which a new procedure had to be manually started. The baseline was measured for each supporting electrolyte in the correct concentration beforehand.

Before each measurement, the desired temperature difference was set to the thermostats. The cell-halves, along with the tubes and cuvette, were filled with the studied solution, so that the initial concentration c_0 was uniform throughout the system. The total volume of the side connected to the flow-through cuvette was measured $V_0^{\alpha} \approx$ 5.0 mL, and the volume of the other half cell $V_0^{\beta} =$ 3.0 mL.

4. Results and discussion

The sign of the Soret coefficient $\sigma^*_{T,23}$ of the polyelectrolyte in the ternary mixture determines whether thermophobic or thermophilic behavior is observed. Fig. 3 shows the time evolution of its concentration in the cold chamber with $\sigma^*_{T,23}$ varying from positive (thermophobic) to negative values (thermophilic). Such a change in $\sigma^*_{T,23}$ could, in principle, be achieved through changes in the Soret coefficient $\sigma_{T,13}$ of the supporting electrolyte, see eq (5). The Soret coefficients of electrolytes usually range between $0–15 \times 10^{-3}$ K^{-1} but also negative coefficient values are found. These coefficients generally increase with temperature [13] and decrease as a function of concentration in dilute solutions [35]. In higher concentrations the Soret coefficient increases again [36,37]. Therefore, a trace electrolyte might show strongly thermophobic behavior in certain

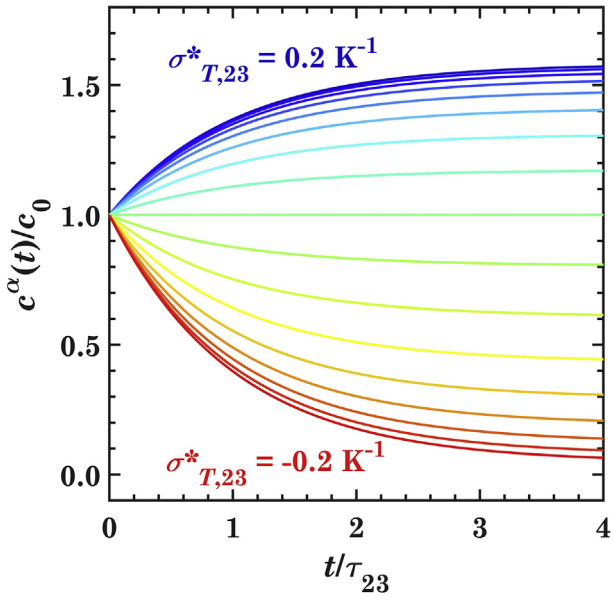

Fig. 3. Simulated thermodiffusion of Na_{2400}PSS. The concentration on the cold side (α) changes when a temperature difference $\Delta T = 20$ K is applied. Depending on its effective Soret coefficient $\sigma^*_{T,23} = 0.2$ K^{-1} … -0.2 K^{-1}, the polyelectrolyte either accumulates at the cold side (thermophobic behavior, blue), or is depleted from the cold side (thermophilic behavior, red). Time is normalized with relaxation time τ_{23} to help comparison, $\omega = 0$. (For interpretation of the references to colour in this figure legend, the reader is referred to the Web version of this article.)

supporting electrolyte concentration, very little tendency for thermodiffusion in another concentration, and upon a change in the supporting electrolyte, reverse into strongly thermophilic behavior. The Soret coefficients of the different species present in multicomponent systems, combined with the different concentration and temperature dependence of these coefficients, might come a long way to explain the apparently inconsistent results obtained in different studies on thermodiffusion and thermophoresis in electrolyte mixtures. Alas, the often non-ideal nature of these systems mean that making accurate predictions from results in binary systems might be cumbersome.

Thermodiffusion of Na_{2400}PSS was studied experimentally in 0.1 mol L^{-1} NaCl supporting electrolyte at $T_{avg} = 308$ K with $\Delta T =$ 20 K. The measured polyelectrolyte concentration in the experimentally-analyzed, cold α-side increases with time (Fig. 4), which indicates that $\sigma^*_{T,23}$ is positive. The extent of thermodiffusion significantly decreases with increasing initial polyelectrolyte concentration. In 12 nmol L^{-1}, the separation between α-side and β-side is almost complete, whereas already in 18 nmol L^{-1}, the separation is much less drastic, and in 68 nmol L^{-1}, the separation is almost zero. The blue lines in Fig. 4 represent best fits to eq (11) with parameters $\sigma^*_{T,23}$, ω and τ_{23} (Table 1).

The observed separation induced by the temperature difference and, hence, the Soret coefficient $\sigma^*_{T,23}$ of the polyelectrolyte in the mixture are strongly dependent on the polyelectrolyte concentration (Fig. 5). In initial concentrations $c_0 < 20$ nmol L^{-1}, $\sigma^*_{T,23}$ increases sharply with decreasing c_0, from values close to zero to values resulting in almost complete depletion of the polyelectrolyte from the hot β-side and enrichment in the cold α-side. From the values of $\sigma^*_{T,23}$ in Table 1 and its concentration dependence, the theoretical steady-state concentration in the cold side is calculated with eq (12) (Fig. 5b).

Qualitatively similar behavior was theoretically predicted in Ref. [29]. The authors measured the Soret coefficients of aqueous Na_{340}PSS ($M \approx 70$ kg/mol) and predicted that in a ternary Na_{340}PSS–NaCl system, a stark thermal separation for the polyelectrolyte could be observed. The Soret coefficient of the polyelectrolyte in the absence of supporting electrolyte would be $\sigma_{T,23} = 5.2 \times 10^{-3}$ K^{-1} while in the presence of the supporting electrolyte it would be over two orders of magnitude larger, $\sigma^*_{T,23} =$ 0.84 K^{-1}. Equation (5) explains this observation because the effective charge $-\nu_{3,2}$ of the polyelectrolyte ion ($C^{-\nu_{3,2}}$) can be very large and then $\sigma^*_{T,23}$ is much larger than $\sigma_{T,23}$.

In principle, eq (5) could be used to estimate the Soret coefficient

$$\sigma_{T,23} = \frac{\sigma^*_{T,23} + \nu_{3,2}\sigma_{T,13}}{1 + \nu_{3,2}} \tag{14}$$

of the Na_{2400}PSS polyelectrolyte in the absence of NaCl from the values $\sigma^*_{T,23}$ measured in the electrolyte mixture and the Soret coefficient $\sigma_{T,13} = 2.3 \times 10^{-3}$ K^{-1} of NaCl (at $T_{avg} = 308$ K and $c_{13} = 0.1$ mol L^{-1}, estimated from concentration dependence reported in Ref. [36] and temperature dependence reported in Ref. [13]). However, it should be noticed that $\nu_{3,2}$ in eq (14) should not be the stoichiometric value $\nu_{3,2} \approx 2400$ but much smaller, representing the effective charge of the PSS anion during electrodiffusion. Thus, for instance, for a 10% of effectively-ionized sulfonate groups [38], a value $\nu_{3,2} \approx 240$ should be used in eq (14). The corresponding estimations of $\sigma_{T,23}$ (Fig. 5c) range from $\sigma_{T,23} = 3.1 \times 10^{-3}$ K^{-1} at the lowest Na_{2400}PSS concentration to

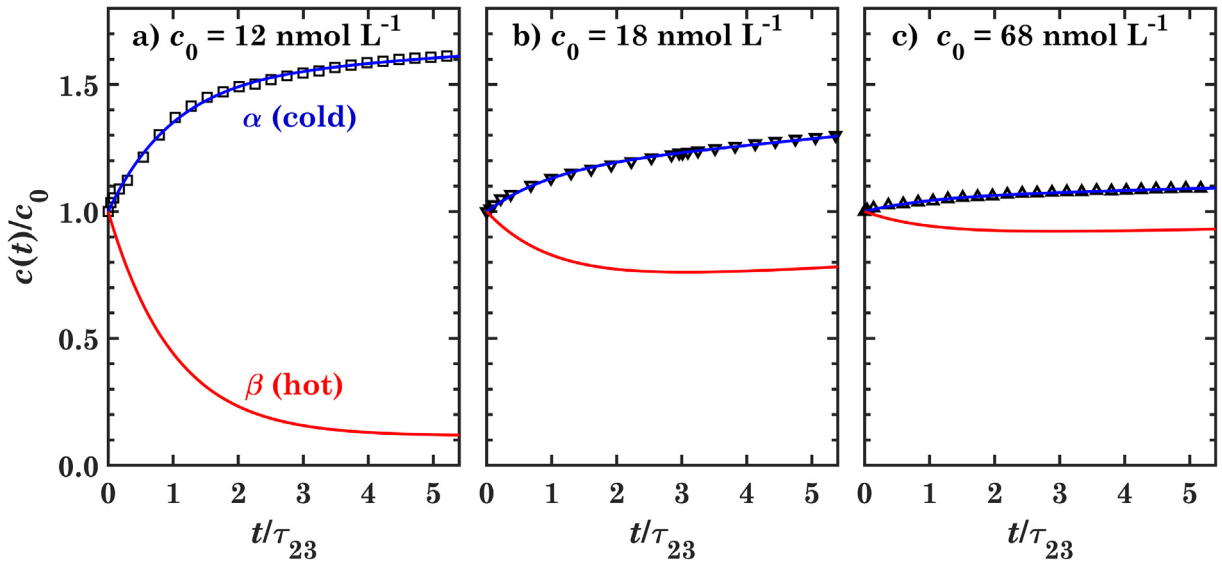

Fig. 4. Thermodiffusion of Na_{2400}PSS in 0.1 mol L^{-1} NaCl at T_{avg} = 308 K with ΔT = 20K and a) c_0 = 12 nmol L^{-1} (6 mg L^{-1}), b) c_0 = 18 nmol L^{-1} (9 mg L^{-1}), and c) c_0 = 68 nmol L^{-1} (34 mg L^{-1}). Symbols represent experimental values. Blue lines (cold α-side) are best fits to eq (11) with the parameters shown in Table 1 and red lines represent eq (10) (hot β-side). The effect of a larger evaporation rate is noticeable in panel b), as the concentration in both chambers increase with time at larger times; note that the relaxation time τ_{23} depends on c_0. (For interpretation of the references to colour in this figure legend, the reader is referred to the Web version of this article.)

Table 1
Fitting parameters for thermodiffusion of Na_{2400}PSS in 0.1 mol L^{-1} NaCl at T_{avg} = 308 K with ΔT = 20 K in various concentrations.

c_0/(nmol L^{-1})	$10^3\sigma^*_{T,23}$ /K^{-1}	$10^7\omega$ / s^{-1}	τ_{23} /h
7	200	2.01	40.9
12	130	1.26	20.4
15	13	2.01	28.8
18	25	2.98	16.1
22	8.0	1.12	9.35
31	5.5	2.61	15.0
43	12	0.835	71.4
46	1.7	0.876	13.3
68	8.1	0.365	43.7
102	−0.10	0.865	4.92

$\sigma_{T,23} = 2.3 \times 10^{-3}$ K^{-1} at the largest concentration. It does not escape our attention that the latter value is too similar to $\sigma_{T,13}$. Table 1 shows a trend of decreasing $\sigma^*_{T,23}$ with increasing Na_{2400}PSS concentration. At large concentrations $\sigma^*_{T,23}$ is so small that eq (14) gives an unrealistic estimation $\sigma_{T,23} \approx \sigma_{T,13}$; in fact, the uncertainty of $\sigma^*_{T,23}$ at 102 nmol L^{-1} is also large. Nevertheless, the estimations of $\sigma_{T,23}$ in Fig. 5c show that $\sigma_{T,23}$ is much smaller than $\sigma^*_{T,23}$, in agreement with the results in Ref. [29], and has a much weaker concentration dependence.

Comparing further with the results from Ref. [29], it is seen that the Soret coefficient for a 70 kg/mol polyelectrolyte is larger than what is reported here for a 500 kg/mol polyelectrolyte. Although this seems counterintuitive, similar results have been reported previously, albeit for a different polyelectrolyte. Lobo and Teixeira

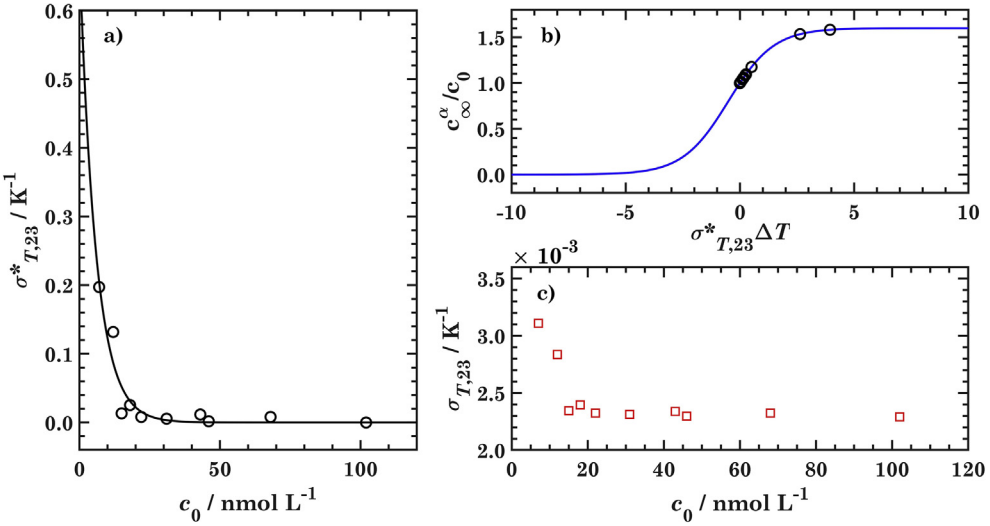

Fig. 5. a) $\sigma^*_{T,23}$ as a function of the initial concentration of the polyelectrolyte in 0.1 mol L^{-1} NaCl (circles), black line an exponential fit to guide the eye. b) Theoretical steady-state concentration of the (cold) α-side as a function of $\sigma^*_{T,23}\Delta T$ (line) and the values (circles) calculated from $\sigma^*_{T,23}$ in panel a. c) Estimated Soret coefficient for the polyelectrolyte in the absence of supporting electrolyte.

[28] reported that the Soret coefficients of sodium polyacrylates of different sizes increased linearly with size up to c. a. 1000 monomer units, but then decreased for larger polyacrylates. These results together would then indicate that the size dependence of polyelectrolyte Soret coefficients is seemingly erratic and not satisfactorily explained by any present theory.

The reported finding that the thermal separation becomes more significant in low concentrations is understood with the present analysis as a result of a slight change in the Soret coefficient of the polyelectrolyte. The concentration dependence of the Soret coefficient found in this study (or the lack thereof) can be perhaps more easily explained if ionic Soret coefficients are considered, although their values cannot be determined individually without a convention of some kind. The Soret coefficient of the polyelectrolyte can be expressed, in an ideal case, as the number-weighted average of the Soret coefficients of its ionic constituents (see Appendix)

$$\sigma_{T,23} = \frac{\sigma_{T,2} + \nu_{3,2}\sigma_{T,3}}{1 + \nu_{3,2}}. \tag{15}$$

Then, if the Soret coefficients of the two ionic species are of the same order of magnitude, the Soret coefficient of the polyelectrolyte is mainly determined through the contribution from the sodium ions ($\nu_{3,2} \gg 1$). Although the concentration of the polyelectrolyte changes, the concentration of sodium ions in the system remains practically constant, as it is dominated by the supporting electrolyte. Similarly, an often reported dependence of the Soret coefficient and ionic strength should yield an almost constant value, as the supporting electrolyte is likely to dominate the ionic strength as well. However, how a polyelectrolyte contributes to ionic strength is not totally unambigious. Furthermore, whether the change in the Soret coefficient is purely down to polyelectrolyte activity changes, or the result of some other phenomenon, such as conformation changes, remains unclear. It should be noted that as the supporting electrolyte Soret coefficient in the experimental conditions used here is merely an estimate, placing too much emphasis on the numerical values should be avoided. The conclusion from Fig. 5 is rather that the estimated Soret coefficient of the polyelectrolyte in the absence of supporting electrolyte is similar to that of the supporting electrolyte, and in very low concentrations, it increases slightly. However, its Soret coefficient and its thermal separation in the ternary mixture are very large.

To verify the role of the supporting electrolyte in the thermodiffusion of polyelectrolytes, Fig. 6a compares the experimental results in four supporting electrolytes: NaCl, $NaClO_4$, Na_2SO_4, and LiCl. LiCl was chosen because of its atypical thermophobic behavior, as its Soret coefficient is close to zero [14]. However, it should be noted that the theory presented here strictly applies only for a ternary system. To highlight the effect of the supporting electrolyte, Fig. 6b shows calculated concentration profiles without the effect of evaporation. These experimental results and calculations show that the supporting electrolyte clearly affects the thermodiffusion of the polyelectrolyte.

The fits of the experimental results in Fig. 6a–eq (11) give the values of the parameters $\sigma^*_{T,23}$, τ_{23} and ω. The Soret coefficient of the polyelectrolyte in NaCl and LiCl is nearly the same $\sigma^*_{T,23} \approx 0.130\,\mathrm{K}^{-1}$, in Na_2SO_4 the value is $0.060\,\mathrm{K}^{-1}$ and in $NaClO_4$ it is $0.030\,\mathrm{K}^{-1}$. In all cases $\sigma^*_{T,23}$ is larger than the estimated values $\sigma_{T,23}$ in absence of supporting electrolyte shown in Fig. 5c. This is considered to indicate that $\sigma_{T,13} < \sigma_{T,23}$. On the contrary, if the supporting electrolyte had a Soret coefficient $\sigma_{T,13} > \sigma_{T,23}$, then it would decrease the Soret coefficient of the trace polyelectrolyte, $\sigma^*_{T,23} < \sigma_{T,23}$ (see eq (5)), and hence decrease the tendency for thermal separation.

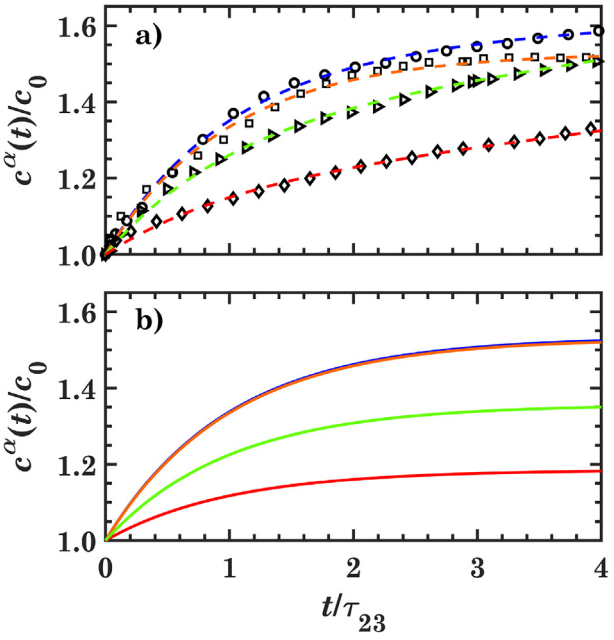

Fig. 6. Thermodiffusion of $Na_{2400}PSS$ ($c_{23} \approx 10$ nmol L^{-1}, $T_{avg} = 308$ K, $\Delta T = 20$ K) in different 0.1 mol L^{-1} supporting electrolytes. a) Experimental results are represented with symbols and dash lines are the best fits: NaCl (circles and blue), LiCl (squares and orange), Na_2SO_4 (triangles and green), and $NaClO_4$ (diamonds and red). b) Theoretical predictions without the effect of evaporation, i.e. $\omega = 0$. Note that the difference between NaCl and LiCl is small and the curves practically overlap. (For interpretation of the references to colour in this figure legend, the reader is referred to the Web version of this article.)

5. Conclusions

The effect of polyelectrolyte concentration and the effect of supporting electrolyte to the thermodiffusion of sodium polystyrene sulfonate in supporting electrolyte was experimentally studied. The glass frit used to separate the two compartments had small pores and a low porosity, which prevented mixing of the two compartments, but we cannot be certain that convection is fully eliminated. Thermodiffusion was observed to be strongly dependent on the concentration of the polyelectrolyte. With very dilute solutions, almost complete separation was observed, *viz* the polyelectrolyte was depleted from the hot side and accumulated to the cold side. In moderately higher concentrations, the separation was significantly weaker. According to our interpretation of the results, however, the change in separation is the result of only small changes in the Soret coefficient of the polyelectrolyte (i.e, in the value estimated in the absence of supporting electrolyte).

In a mixture of electrolytes, the electrolyte that has a higher Soret coefficient (in the absence of the other electrolyte) shows an even higher Soret coefficient when forming the mixture [39]. Our experimental observations confirm that the supporting electrolyte facilitates the thermodiffusion of the polyelectrolyte. The theory predicts that this effect is particularly important for a trace electrolyte. The measured Soret coefficient of the polyelectrolyte in the mixture is indeed very large at low polyelectrolyte concentrations.

Similarly, in a mixture of electrolytes, the electrolyte that has a lower Soret coefficient (in the absence of the other electrolyte) shows an even lower Soret coefficient in the mixture, and the theory predicts that it might even reverse its sign. For the case of a trace polyelectrolyte in a supporting electrolyte, this means that if the Soret coefficient of the polyelectrolyte alone were lower than that of the supporting electrolyte alone, then the Soret coefficient of the polyelectrolyte in the mixture could be reduced. Our

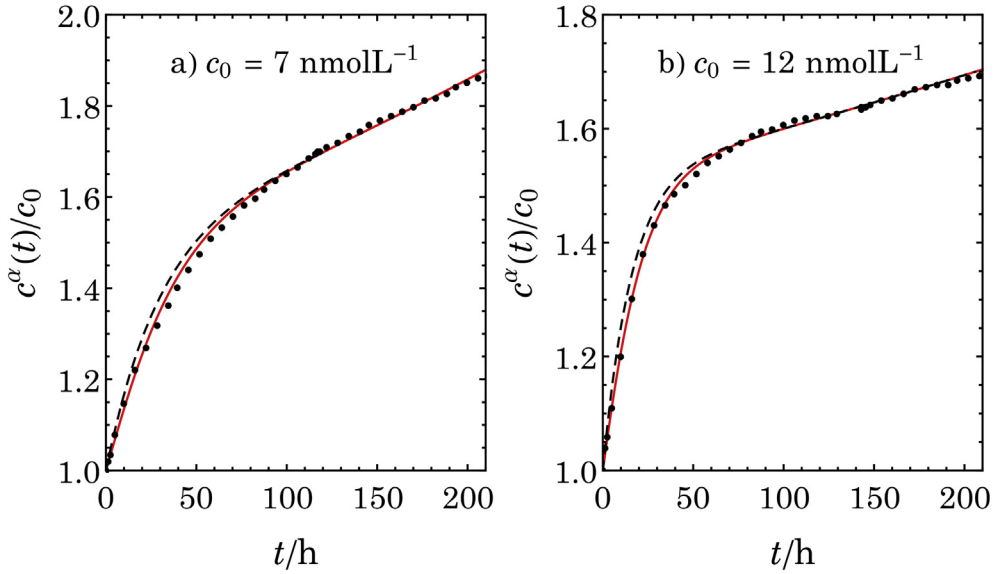

Fig. 7. Since the supporting electrolyte diffuses faster than the polyelectrolyte, it seems reasonable for the sake of simplicity to assume that the former has reached the Soret equilibrium distribution while $Na_{2400}PSS$ is still thermodiffusing. The symbols are experimental measurements of $c^\alpha_{23}(t)$. The solid lines show $c^\alpha_{23}(t)$ from the exact numerical solution of the transport equations of the polyelectrolyte and the dashed lines from the approximate solution based on $J_{13} \approx 0$ (for the same parameter values). In all curves we have used $\sigma_{T,13} = 2.3 \times 10^{-3}$ K^{-1}, $\sigma_{T,23} = 3.8 \times 10^{-3}$ K^{-1}, $\nu_{3,2} = 360$ and $V_0^\alpha = 5.8$ mL. Other parameter values are: a) $\tau_{23} = 27.9$ h and $\omega = 2.55 \times 10^{-7}$s^{-1}; b) $\tau_{23} = 15.6$ h and $\omega = 1.45 \times 10^{-7}$s^{-1}. The values of $\sigma^*_{T,23}$ can be calculated using eq (5).

experiments with different supporting electrolytes show a clear effect on the thermodiffusion of the polyelectrolyte in the mixture. However, positive Soret coefficients are always observed, which seems to indicate that the supporting electrolytes used all have lower Soret coefficient than the polyelectrolyte (in the absence of supporting electrolyte). The polyelectrolyte separated most strongly in NaCl and LiCl, and most weakly in $NaClO_4$. The results indicate that the effect of the supporting electrolyte has to be properly taken into account when analyzing thermodiffusion or thermophoresis in multicomponent systems, such as protein or DNA in biological buffers.

Polyelectrolytes being notoriously difficult to model due to their inherently complex nature, the theory most likely needs improvements, such as activity corrections. We do not know the precise effective charge of the polyelectrolyte or how strongly the counter-ions are attached to the polyelectrolyte, and how they contribute to the Soret coefficient of the polyelectrolyte. The contribution of polyelectrolyte to the ionic strength of the solution is another important unknown, as Soret coefficient has been shown to be a function of ionic strength. Furthermore [28], suggested that also the structure of the polyelectrolyte might be an important issue, as larger polyelectrolytes are likely to overlap with themselves, resulting in lower Soret coefficient values. Yet, the results of this paper offer new and interesting insight into the thermodiffusion of polyelectrolytes, and the theory proposed in this paper could be used as a starting point for a more thorough theoretical description of the thermodiffusion in supporting electrolytes.

Acknowledgements

MJ wishes to acknowledge Emil Aaltonen Foundation (grant number 180066), Waldemar von Frenckells Foundation, Kaute Foundation, and Aalto University School of Chemical Engineering for financial support. JAM acknowledges the support from European Regional Development Funds and Ministerio de Ciencia, Innovación y Universidades under project PGC2018-097359-B-100.

Appendix

In the Nernst-Planck approximation for isothermal electrodiffusion [33], the molar flux density of ionic species i is $-\vec{j}_i = l_{i,i}\vec{\nabla}\tilde{\mu}_i$, where $\vec{\nabla}\tilde{\mu}_i = RT\vec{\nabla}\ln c_i + z_i F\vec{\nabla}\varphi$, R is the molar gas constant, T the temperature, φ the electric potential, F the Faraday constant, c_i the concentration of species i, z_i its charge number, $l_{i,i} = D_i c_i/RT = t_i\kappa/(z_i^2F^2)$ its phenomenological transport coefficient, D_i its diffusion coefficient, $t_i = z_i^2 D_i c_i/\sum_k z_k^2 D_k c_k$ its transport number, and κ is the electrical conductivity. In non-isothermal electrodiffusion, this flux density is

$$-\vec{j}_i = D_i c_i\left(\sigma_{T,i}\vec{\nabla}T + \vec{\nabla}\ln c_i + z_i\frac{F}{RT}\vec{\nabla}\varphi\right) \tag{A1}$$

where $\sigma_{T,i}$ is the intrinsic Soret coefficient of species i [2,39,40]. When the current density $\vec{I} = F\sum_i z_i\vec{j}_i$ is zero, the thermodiffusion electric potential gradient is

$$\begin{aligned}-\frac{F}{RT}\vec{\nabla}\varphi_{I=0} &= \sum_i \frac{t_i}{z_i}\left(\sigma_{T,i}\vec{\nabla}T + \vec{\nabla}\ln c_i\right)\\ &= \sum_i \frac{t_i\sigma_{T,i}}{z_i}\vec{\nabla}T + \frac{t_1}{z_1^2 D_1 c_1}\sum_i z_i D_i\vec{\nabla}c_i\end{aligned} \tag{A2}$$

Under equilibrium conditions, $j_i = 0$, this gradient is [39]

$$-\frac{F}{RT}\vec{\nabla}\varphi_{j_i=0} = \frac{\sum_j z_j c_j\sigma_{T,j}}{\sum_k z_k^2 c_k}\vec{\nabla}T \tag{A3}$$

where we have used $\sum_j z_j\vec{j}_j/D_j = \vec{0}$ and the local electroneutrality condition in the form $\sum_j z_j\vec{\nabla}c_j = \vec{0}$. Inserting eq (A3) in eq (A1) for $j_i = 0$ leads to $\vec{\nabla}\ln c_i = -\sigma^*_{T,i}\vec{\nabla}T$, where

$$\sigma^*_{T,i} = \sigma_{T,i} - z_i \frac{\sum_j z_j c_j \sigma_{T,j}}{\sum_k z_k^2 c_k} \tag{A4}$$

is the so-called "observed" Soret coefficient of ionic species i [39]. In a binary electrolyte $A_{\nu_1}C_{\nu_{3,1}}$ (index 13), eq (A4) reduces to $\sigma^*_{T,1} = \sigma^*_{T,3} = \sigma_{T,13}$ where $\sigma_{T,13} = (\nu_1\sigma_{T,1} + \nu_{3,1}\sigma_{T,3})/(\nu_1 + \nu_{3,1})$ is the Soret coefficient of this electrolyte, as the ionic concentrations are $c_1 = \nu_1 c_{13}$ and $c_3 = \nu_{3,1} c_{13}$ and $z_1\nu_1 + z_3\nu_{3,1} = 0$.

In a mixture of electrolytes $A_{\nu_1}C_{\nu_{3,1}}$ (13) and $B_{\nu_2}C_{\nu_{3,2}}$ (23) sharing a common ion, the electrolyte concentrations are c_{13} and c_{23}, and the ionic concentrations are $c_1 = \nu_1 c_{13}$, $c_2 = \nu_2 c_{23}$, and $c_3 = \nu_{3,1} c_{13} + \nu_{3,2}\, c_{23}$. The equations $\vec{\nabla}\ln c_1 = -\sigma^*_{T,1}\vec{\nabla}T$ and $\vec{\nabla}\ln c_2 = -\sigma^*_{T,2}\vec{\nabla}T$ describing the ionic concentration gradients at equilibrium are then equivalent to $\vec{\nabla}\ln c_{13} = -\sigma^*_{T,13}\vec{\nabla}T$ and $\vec{\nabla}\ln c_{23} = -\sigma^*_{T,23}\vec{\nabla}T$. Thus, e.g., the Soret coefficient of electrolyte 23 in the ternary mixture is

$$\sigma^*_{T,23} = \sigma^*_{T,2} = \sigma_{T,23} + \frac{\sigma_{T,23} - \sigma_{T,13}}{\frac{\nu_2}{\nu_{3,2}} + \frac{\nu_1}{\nu_{3,1}}\frac{\nu_2+\nu_{3,2}}{\nu_1+\nu_{3,1}}\frac{c_{23}}{c_{13}}} \tag{A5}$$

where $\sigma_{T,23} = (\nu_2\sigma_{T,2} + \nu_{3,2}\sigma_{T,3})/(\nu_2 + \nu_{3,2})$ is the Soret coefficient of electrolyte 23 in the absence of electrolyte 13. Permutation of indexes 1 and 2 would give the equation for $\sigma^*_{T,13} = \sigma^*_{T,1}$. These equations predict, in agreement with observations [39], that if electrolyte 23 alone has a higher Soret coefficient that electrolyte 13 alone, $\sigma_{T,23} > \sigma_{T,13}$, then electrolyte 23 in the mixture has an even higher Soret coefficient, $\sigma^*_{T,23} > \sigma_{T,23}$; and, similarly, $\sigma^*_{T,13} < \sigma_{T,13}$. The difference of the Soret coefficients of the electrolytes in the mixture $\sigma^*_{T,23} - \sigma^*_{T,13}$ is larger than the difference $\sigma_{T,23} - \sigma_{T,13}$ of the Soret coefficients of the pure electrolytes. In the case of trace electrolyte $c_{23} \ll c_{13}$, eq (A6) reduces to eq (5) in the Theory section and $\sigma^*_{T,13} \approx \sigma_{T,13}$.

In a mixture of electrolytes $A_{\nu_1}C_{\nu_{3,1}}$ (13) and $B_{\nu_2}C_{\nu_{3,2}}$ (23), the electrolyte flux densities are independent of the current density and can be conveniently evaluated from eqs A1 and A2 as $\vec{J}_{13} = \vec{j}_1/\nu_1$ and $\vec{J}_{23} = \vec{j}_2/\nu_2$ when $I = 0$ as

$$\begin{aligned} -\vec{J}_{13} = {} & [(1-t_1)D_1 + t_1 D_3]\vec{\nabla}c_{13} + \frac{\nu_{3,2}}{\nu_{3,1}} t_1 (D_3 - D_2)\vec{\nabla}c_{23} \\ & + D_1 \frac{c_{13}}{\nu_1}\left[(1-t_1)(\nu_1 + \nu_{3,1})\sigma_{T,13} - \frac{\nu_{3,1}}{\nu_{3,2}} t_2 (\nu_2 \right. \\ & \left. + \nu_{3,2})\sigma_{T,23}\right]\vec{\nabla}T \end{aligned} \tag{A6}$$

$$\begin{aligned} -\vec{J}_{23} = {} & \frac{\nu_{3,1}}{\nu_{3,2}} t_2 (D_3 - D_1)\vec{\nabla}c_{13} + [(1-t_2)D_2 + t_2 D_3]\vec{\nabla}c_{23} \\ & + D_2 \frac{c_{23}}{\nu_2}\left[(1-t_2)(\nu_2 + \nu_{3,2})\sigma_{T,23} - \frac{\nu_{3,2}}{\nu_{3,1}} t_1 (\nu_1 \right. \\ & \left. + \nu_{3,1})\sigma_{T,13}\right]\vec{\nabla}T. \end{aligned} \tag{A7}$$

Equation (A7) is the same as eq (2) in the Theory section. When species 2 is a trace ion, so that $t_2 \ll 1$ and $c_{23} \ll c_{13}$, this species does not affect the transport of the supporting electrolyte 13. Then, eqs A6 and A7 reduce to eqs (1) and (3), where $D_{13} = (\nu_1 + \nu_{3,1})D_1 D_3/(\nu_{3,1}D_1 + \nu_1 D_3)$ and $D_{23,13} = (\nu_{3,1}/\nu_{3,2})t_2(D_3 - D_1) \approx \alpha D_2 c_{23}/c_{13}$ with $\alpha = (\nu_1\nu_{3,2}/\nu_2)(D_3 - D_1)/(\nu_{3,1}D_1 + \nu_1 D_3)$.

In the Theory section we have used the approximation $J_{13} \approx 0$ to simplify eq (3) into eq (6). We can justify this approximation by solving eq (A7) for $t_2 \ll 1$,

$$-\frac{\vec{J}_{23}}{D_2} = \vec{\nabla}c_{23} + c_{23}\left[\sigma^*_{T,23}\vec{\nabla}T + \alpha(\vec{\nabla}\ln c_{13} + \sigma_{T,13}\vec{\nabla}T)\right]. \tag{A8}$$

Since it involves $\vec{\nabla}\ln c_{13}$, the function $c_{13}(x,t)$ must be evaluated first. Integration of

$$-\frac{J_{13}}{D_{13}} = \left(\frac{\partial c_{13}}{\partial x}\right)_t + c_{13}\sigma_{T,13}\frac{\Delta T}{h} \tag{A9}$$

with boundary conditions $c_{13}(0) = c^\alpha_{13}$ and $c_{13}(h) = c^\beta_{13}$ gives

$$-\frac{J_{13}}{D_{13}} = \frac{E_{T,13}}{h}\left(c^\beta_{13} - c^\alpha_{13}\mathrm{e}^{-\sigma_{T,13}\Delta T}\right) \tag{A10}$$

where $E_{T,13} = \sigma_{T,13}\Delta T/(1 - \mathrm{e}^{-\sigma_{T,13}\Delta T})$. After elimination of c^β_{13} using eq (9) (from the Theory section), substitution of J_{13} from eq (A10) into eq (8) gives

$$\frac{\mathrm{d}(V^\alpha c^\alpha_{13})}{V^\alpha_0 c^\alpha_{13,\infty} - V^\alpha c^\alpha_{13}} = \frac{1}{\tau_{13}}\frac{\mathrm{d}t}{1 - \omega t}, \tag{A11}$$

where

$$\frac{1}{\tau_{13}} = \frac{AD_{13}E_{T,13}}{h}\left(\frac{\mathrm{e}^{-\sigma_{T,13}\Delta T}}{V^\alpha_0} + \frac{1}{V^\beta_0}\right) \tag{A12}$$

$$c^\alpha_{13,\infty} = \frac{V^\alpha_0 + V^\beta_0}{V^\alpha_0 + V^\beta_0 \mathrm{e}^{-\sigma_{T,13}\Delta T}} c_{13,0}. \tag{A13}$$

The integration of eq (A11) is

$$c_{13}(x,t) \approx \frac{c^\alpha_{13,\infty}\mathrm{e}^{-\sigma_{T,13}\Delta T(x/h)} + \left(c_{13,0} - c^\alpha_{13,\infty}\mathrm{e}^{-\sigma_{T,13}\Delta T(x/h)}\right)(1-\omega t)^{1/(\omega\tau_{13})}}{1 - \omega t}. \tag{A14}$$

Thus, the concentration $c_{13}(x,t)$ inside the membrane changes from its initial value $c_{13,0}$ to $c^\alpha_{13,\infty}\mathrm{e}^{-\sigma_{T,13}\Delta T(x/h)}/(1-\omega t)$ at times t so that $\omega\tau_{13} \ll \omega t \ll 1$.

Equation A8 is

$$-\frac{J_{23}(t)}{D_2} = \left(\frac{\partial c_{23}}{\partial x}\right)_t + F(x,t)c_{23}(x,t), \tag{A15}$$

where $F(x,t) = (\sigma^*_{T,23} + \alpha\sigma_{T,13})\Delta T/h + \alpha(\partial\ln c_{13}/\partial x)_t$ and $J_{23}(t)$ is independent of x in the quasi-steady state approximation. The integration of eq (A15) with respect to x under the boundary conditions $c_{23}(0,t) = c^\alpha_{23}(t)$ and $c_{23}(h,t) = c^\beta_{23}(t)$ gives

$$\frac{J_{23}(t)}{D_{23}} = \frac{c^\beta_{23} - c^\alpha_{23}(t)\exp\left(-\int_0^h F(x,t)\mathrm{d}x\right)}{\int_0^h \exp\left(-\int_x^h F(u,t)\mathrm{d}u\right)\mathrm{d}x}. \tag{A16}$$

Using eq (9) to eliminate c^β_{23}, substitution of J_{23} from eq (A16) in eq (8) for electrolyte 23 leads to a differential equation describing the time variation of $c^\alpha_{23}(t)$ which can be integrated numerically. Fig. 7 shows the transients obtained from this numerical integration and

their comparison with the theoretical curves obtained from eq (11), that is, using the approximation of Soret equilibrium for the supporting electrolyte $J_{13} \approx 0$. The objective of this comparison is to justify the validity of the latter approximation (dashed line) and not to obtain the values of fitting parameters. Nevertheless, the values given to parameters are such that the functions $c_{23}^{\alpha}(t)$ obtained from the numerical simulation (solid line) closely follow the experimental measurements (symbols). Given the complexity of both the measurements and the theoretical analysis, having eq (12) the same functional shape as experimentally observed, and noticing the small differences evidenced in Fig. 7, we can conclude that the approximation $J_{13} \approx 0$ is justified, especially in long measurements.

References

[1] J.N. Agar, Thermogalvanic cells, in: P. Delahay (Ed.), Advances in Electrochemistry and Electrochemical Engineering, Interscience, New York, 1963, pp. 31–120.

[2] R. Haase, *Thermodynamics of Irreversible Processes*, Dover Publications, Inc., Mineola, 1990.

[3] S. Duhr, D. Braun, Why molecules move along a temperature gradient, Proc. Natl. Acad. Sci. U.S.A. 103 (2006) 19678–19682, https://doi.org/10.1073/pnas.0603873103.

[4] S. Iacopini, R. Rusconi, R. Piazza, The "macromolecular tourist": universal temperature dependence of thermal diffusion in aqueous colloidal suspensions, Eur. Phys. J. E: Soft Matter Biol. Phys. 19 (2006) 59–67, https://doi.org/10.1140/epje/e2006-00012-9.

[5] R.A. Sperling, T. Liedl, S. Duhr, S. Kudera, M. Zanella, C.A.J. Lin, W.H. Chang, D. Braun, W.J. Parak, Size determination of (bio)conjugated water-soluble colloidal nanoparticles: a comparison of different techniques, J. Phys. Chem. C 111 (2007) 11552–11559, https://doi.org/10.1021/jp070999d.

[6] R. Piazza, Thermal forces": colloids in temperature gradients, J. Phys. Condens. Matter 16 (2004) S4195–S4211, https://doi.org/10.1088/0953-8984/16/38/032.

[7] P. Reineck, C.J. Wienken, D. Braun, Thermophoresis of single stranded DNA, Electrophoresis 31 (2010) 279–286, https://doi.org/10.1002/elps.200900505.

[8] S. Iacopini, R. Piazza, Thermophoresis in protein solutions, Europhys. Lett. 63 (2003) 247–253, https://doi.org/10.1209/epl/i2003-00520-y.

[9] D.R. Caldwell, S.A. Eide, Separation of seawater by Soret diffusion, Deep Sea Res. Part A 32 (1985) 965–982, https://doi.org/10.1016/0198-0149(85)90039-1.

[10] D. Braun, A. Libchaber, Trapping of DNA by thermophoretic depletion and convection, Phys. Rev. Lett. 89 (2002) 188103, https://doi.org/10.1103/PhysRevLett.89.188103.

[11] M. Kreysing, L. Keil, S. Lanzmich, D. Braun, Heat flux across an open pore enables the continuous replication and selection of oligonucleotides towards increasing length, Nat. Chem. 7 (2015) 203–208, https://doi.org/10.1038/nchem.2155.

[12] I. Budin, R.J. Bruckner, J.W. Szostak, Formation of protocell-like vesicles in a thermal diffusion column, J. Am. Chem. Soc. 131 (2009) 9628–9629, https://doi.org/10.1021/ja9029818.

[13] J.N. Agar, J.C.R. Turner, Thermal diffusion in solutions of electrolytes, Proc. R. Soc. London, Ser. A 255 (1960) 307–330, https://doi.org/10.1098/rspa.1960.0070.

[14] P.N. Snowdon, J.C.R. Turner, The Soret effect in some 0.01 normal aqueous electrolytes, Trans. Faraday Soc. 56 (1960) 1409–1418, https://doi.org/10.1039/TF9605601409.

[15] A.L. Sehnem, D. Niether, S. Wiegand, A.M. Figueiredo Neto, Thermodiffusion of monovalent organic salts in water, J. Phys. Chem. B 122 (2018) 4093–4100, https://doi.org/10.1021/acs.jpcb.8b01152.

[16] J.K. Platten, M.M. Bou-Ali, J.F. Dutrieux, Enhanced molecular separation in inclined thermogravitational columns, J. Phys. Chem. B 107 (2003) 11763–11767, https://doi.org/10.1021/jp034780k.

[17] A. Leahy-Dios, A. Firoozabadi, Molecular and thermal diffusion coefficients of alkane-alkane and alkane-aromatic binary mixtures: effect of shape and size of molecules, J. Phys. Chem. B 111 (2007) 191–198, https://doi.org/10.1021/jp064719q.

[18] P. Blanco, P. Polyakov, M. Mounir Bou-Ali, S. Wiegand, Thermal diffusion and molecular diffusion values for some alkane mixtures: a comparison between thermogravitational column and thermal diffusion forced Rayleigh scattering, J. Phys. Chem. B 112 (2008) 8340–8345, https://doi.org/10.1021/jp801894b.

[19] R. Kita, S. Wiegand, J. Luettmer-Strathmann, Sign change of the Soret coefficient of poly(ethylene oxide) in water/ethanol mixtures observed by thermal diffusion forced Rayleigh scattering, J. Chem. Phys. 121 (2004) 3874–3885, https://doi.org/10.1063/1.1771631.

[20] J. Rauch, M. Hartung, A.F. Privalov, W. Köhler, Correlation between thermal diffusion and solvent self-diffusion in semidilute and concentrated polymer solutions, J. Chem. Phys. 126 (2007) 214901, https://doi.org/10.1063/1.2738467.

[21] D. Stadelmaier, W. Köhler, From small molecules to high polymers: investigation of the crossover of thermal diffusion in dilute polystyrene solutions, Macromolecules 41 (2008) 6205–6209, https://doi.org/10.1021/ma800891p.

[22] R. Piazza, A. Guarino, Soret effect in interacting micellar solutions, Phys. Rev. Lett. 88 (2002) 208302, https://doi.org/10.1103/PhysRevLett.88.208302.

[23] R. Piazza, A. Parola, Thermophoresis in colloidal suspensions, J. Phys. Condens. Matter 20 (2008) 153102, https://doi.org/10.1088/0953-8984/20/15/153102.

[24] D. Vigolo, S. Buzzaccaro, R. Piazza, Thermophoresis and thermoelectricity in surfactant solutions, Langmuir 26 (2010) 7792–7801, https://doi.org/10.1021/la904588s.

[25] M.E. Schimpf, Thermodiffusion of polymer solutions in convectionless cells, in: W. Köhler, S. Wiegand (Eds.), Thermal Nonequilibrium Phenomena in Fluid Mixtures, Springer, Berlin, 2002, pp. 285–312, https://doi.org/10.1007/3-540-45791-7.

[26] A. Hammack, Y.L. Chen, J.K. Pearce, Role of dissolved salts in thermophoresis of DNA: lattice-Boltzmann-based simulations, Phys. Rev. E: Stat. Nonlin. Soft Matter Phys. 83 (2011), 031915, https://doi.org/10.1103/PhysRevE.83.031915.

[27] J.N. Agar, V.M.M. Lobo, Heats of transport of polyelectrolytes, Electrochim. Acta 20 (1975) 319–320, https://doi.org/10.1016/0013-4686(75)90011-0.

[28] V.M.M. Lobo, M.H.S.F. Teixeira, Soret coefficients of some polyelectrolytes, Electrochim. Acta 27 (1982) 1145–1147, https://doi.org/10.1016/0013-4686(82)80124-2.

[29] D.G. Leaist, L. Hao, Very large thermal separations for polyelectrolytes in salt solutions, J. Chem. Soc. Faraday. Trans. 90 (1994) 1909–1911, https://doi.org/10.1039/FT9949001909.

[30] M. Jokinen, J.A. Manzanares, L. Murtomäki, Soret coefficient of trace ions determined with electrochemical impedance spectroscopy in a thin cell. Theory and measurement, J. Electroanal. Chem. 820 (2018) 67–73, https://doi.org/10.1016/j.jelechem.2018.04.054.

[31] C.W. Carr, K. Sollner, New experiments on thermoosmosis, J. Electrochem. Soc. 109 (1962) 616–622, https://doi.org/10.1149/1.2425508.

[32] M. Dietzel, S. Hardt, Flow and streaming potential of an electrolyte in a channel with an axial temperature gradient, J. Fluid Mech. 813 (2017) 1060–1111, https://doi.org/10.1017/jfm.2016.844.

[33] K. Kontturi, L. Murtomäki, J.A. Manzanares, *Ionic Transport Processes*, Oxford University Press, Oxford, 2008.

[34] PermeGear General Catalog. https://permegear.com/wp-content/uploads/2019/02/PermeGear-Catalog.pdf, 2018. (Accessed 1 February 2019).

[35] P.N. Snowdon, J.C.R. Turner, The concentration dependence of the Soret effect, Trans. Faraday Soc. 56 (1960) 1812–1819, https://doi.org/10.1039/tf9605601812.

[36] M. Jokinen, J.A. Manzanares, K. Kontturi, L. Murtomäki, Thermal potential of ion-exchange membranes and its application to thermoelectric power generation, J. Membr. Sci. 499 (2016) 234–244, https://doi.org/10.1016/j.memsci.2015.10.042.

[37] J. Colombani, J. Bert, J. Dupuy-Philon, Thermal diffusion in (LiCl, RH2O), J. Chem. Phys. 110 (1999) 8622–8627, https://doi.org/10.1063/1.478769.

[38] A.-K. Kontturi, K. Parovuori, Temperature dependence of the diffusion coefficients and effective charge numbers of polystyrenesulfonate. A comparison with lignosulfonate, Acta Chem. Scand. 47 (1993) 529–531, https://doi.org/10.3891/acta.chem.scand.47-0529.

[39] G. Guthrie, J.N. Wilson, V. Schomaker, Theory of the thermal diffusion of electrolytes in a clusius column, J. Chem. Phys. 17 (1949) 310–313, https://doi.org/10.1063/1.1747244.

[40] W.W. Karger, Zur Theorie des Soret-Effekts in Mischungen von Elektrolytlösnungen, Z. Phys. Chem. 5 (1955) 232–239, https://doi.org/10.1524/zpch.1955.5.3_4.232.